Proc. Natl. Acad. Sci. USA
Vol. 93, pp. 2991–2995, April 1996
Biophysics

Thermal unfolding of human high-density apolipoprotein A-1: Implications for a lipid-free molten globular state

(non-two-state transition/differential scanning calorimetry/circular dichroism)

OLGA GURSKY* AND DAVID ATKINSON

Department of Biophysics, Boston University School of Medicine, 80 East Concord Street, Boston, MA 02118

Communicated by Donald L. D. Caspar, Florida State University, Tallahassee, FL, December 18, 1995 (received for review August 24, 1995)

ABSTRACT **Apolipoprotein A-1 (apoA-1) in complex with high-density lipoprotein is critically involved in the transport and metabolism of cholesterol and in the pathogenesis of atherosclerosis. We reexamined the thermal unfolding of lipid-free apoA-1 in low-salt solution at pH ≈7, by using differential scanning calorimetry and circular dichroism. At protein concentrations <5 mg/ml, thermal unfolding of apoA-1 is resolved as an extended peak (25°C–90°C) that can be largely accounted for by a single reversible non-two-state transition with midpoint T_m = 57 ± 1°C, calorimetric enthalpy $\Delta H(T_m)$ = 200 ± 20 kcal/mol (1 kcal = 4.18 kJ), van't Hoff enthalpy $\Delta H_v(T_m) \approx 32.5$ kcal/mol, and cooperativity $\Delta H_v(T_m)/\Delta H(T_m) \approx 0.16$. The enthalpy $\Delta H(T_m)$ can be accounted for by melting of the α-helical structure that is inferred by CD to constitute ≈60% of apoA-1 amino acids. Farand near-UV CD spectra reveal noncoincident melting of the secondary and tertiary structural elements and indicate a well-defined secondary structure but a largely melted tertiary structure for apoA-1 at ≈37°C and pH 7. This suggests a molten globular-like state for lipid-free apoA-1 under near-physiological conditions. Our results suggest that *in vivo* lipid binding by apoA-1 may be mediated via the molten globular apolipoprotein state in plasma.**

Apolipoprotein A-1 [apoA-1; 28 kDa, 243 amino acids of known sequence (1, 2)] is the major protein of high density lipoprotein (HDL) particles. In complex with HDL, apoA-1 mediates reverse cholesterol transport and metabolism (3) and acts as a cofactor for the enzyme lecithin:cholesterol acyltransferase (4). The levels of apoA-1 and HDL in human plasma correlate inversely with the probability of developing atherosclerosis (5). The sequences of apoA-1 and other exchangeable apolipoproteins contain characteristic 22-residue tandem repeats (6) predicted to form amphiphatic α-helixes that are proposed to play the key role in the lipid binding (7, 8). Long (19–35 amino acids) amphiphatic α-helices packed in elongated bundles have been observed in two apolipoprotein x-ray crystal structures (9, 10). CD analysis indicates ≈85% α-helical content for apoA-1 on HDL, compared to ≈60% in the lipid-free form (11) that is inferred to have a compact prolate shape (12). In plasma, apoA-1 is in dynamic equilibrium among a variety of expanded conformations adopted on nascent discoidal and spherical HDL (13). The conformation of apoA-1 varies with the size and composition of HDL, providing an important determinant of HDL metabolism (14). Thus, both the lipid binding and the functions of apoA-1 on HDL are critically dependent on its conformational adaptability.

The thermodynamic properties of apoA-1 unfolding appear different from that of typical globular proteins. Chemical unfolding of apoA-I is brought about by only ≈1 M guanidine hydrochloride (15) or 1.5 M urea (16). A previous analysis of the thermal unfolding of lipid-free apoA-1 using low-sensitivity calorimetry led to an estimate of the free energy of stabilization $\Delta G(37°C) \approx 2.4$ kcal/mol (1 kcal = 4.18 kJ) (16, 17), compared to 5–15 kcal/mol typical for globular proteins. Similar low ΔG was inferred from the spectroscopic analysis of apoA-1 denaturation on the assumption of two-state kinetics (16). However, this assumption may not be valid, as suggested by the spectroscopic analysis of the chemical denaturation of apoA-1 in the course of which stable unfolding intermediates were detected (15, 18).

Our work revises the thermodynamic description of apoA-1 unfolding under near-physiological conditions. By using adiabatic differential scanning calorimetry and far- and near-UV CD, we demonstrate that lipid-free apoA-1 undergoes a low-cooperativity non-two-state thermal unfolding and displays other properties consistent with the molten globular state. The molten globular state is defined as a compact folding intermediate with a near-native secondary structure but lax tertiary structure (19, 20). Our results suggest that apoA-1 may perform its major physiological function, namely lipid binding, via the molten globular state in plasma.

MATERIALS AND METHODS

Protein Preparation. ApoA-1, which was isolated and purified from human plasma HDL as described (21), migrated as a single band on SDS/10% polyacrylamide gels. The protein was dissolved in 8 M urea and refolded by subsequent dialysis against guanidine hydrochloride solutions of 6 M, 4 M, and 2 M concentrations, followed by extensive dialysis against the appropriate buffer (10 mM sodium phosphate, carbonate, or Hepes with 0.02% NaN_3 at pH 7.2). The protein prepared by this method has been shown to retain full biological activity (21). Protein concentrations were determined by a modified chromatographic Lowry assay (22) and by UV absorption at 280 nm.

Differential Scanning Calorimetry. The heat capacity $C_p(T)$ of degassed samples containing protein at concentrations of 1.7–8.0 mg/ml and/or buffer was recorded over a temperature range of 5°C–105°C by using a high-resolution differential scanning calorimeter, MC-2 (Microcal, Amherst, MA). Repeatability of the data was assessed by comparing the endotherms recorded from the same sample in a series of consecutive heatings from 5°C to gradually increasing temperatures (35°C, 45°C, . . . 105°C), each followed by an equilibration at 5°C. Reversibility (or equilibrium character) of the transition was assessed by comparing endotherms recorded from the same sample with scanning rates 45°C and 90°C per hour. According to these criteria, apoA-1 unfolding is reversible and repeatable in the temperature range of 5°C–65°C. Heating above 65°C leads to heat capacity differences between consecutive scans (Fig. 1 *Inset*) that increase as the time of the protein incubation at elevated temperatures is increased. These irreversible changes (which may reflect chemical mod-

The publication costs of this article were defrayed in part by page charge payment. This article must therefore be hereby marked "*advertisement*" in accordance with 18 U.S.C. §1734 solely to indicate this fact.

Abbreviations: apoA-1, apolipoprotein A-1; HDL, high density lipoprotein.

*To whom reprint requests should be addressed.

ifications to the thermally denatured protein) occur on a slower time scale than the protein unfolding and constitute only ≈15% of the total calorimetric enthalpy (Fig. 2). Thus, these high-temperature irreversible changes do not preclude equilibrium thermodynamic analysis of apoA-1 unfolding.

The buffer–buffer baselines were subtracted from the protein–buffer data that were analyzed subsequently with the Microcal ORIGIN software package. Integration of the $C_p(T)$ peak [that extends from 25°C to 90°C with the peak temperature $T_m \approx 57$°C (Fig. 2)] was carried out by using cubic baseline extrapolation of the portions of the data recorded at

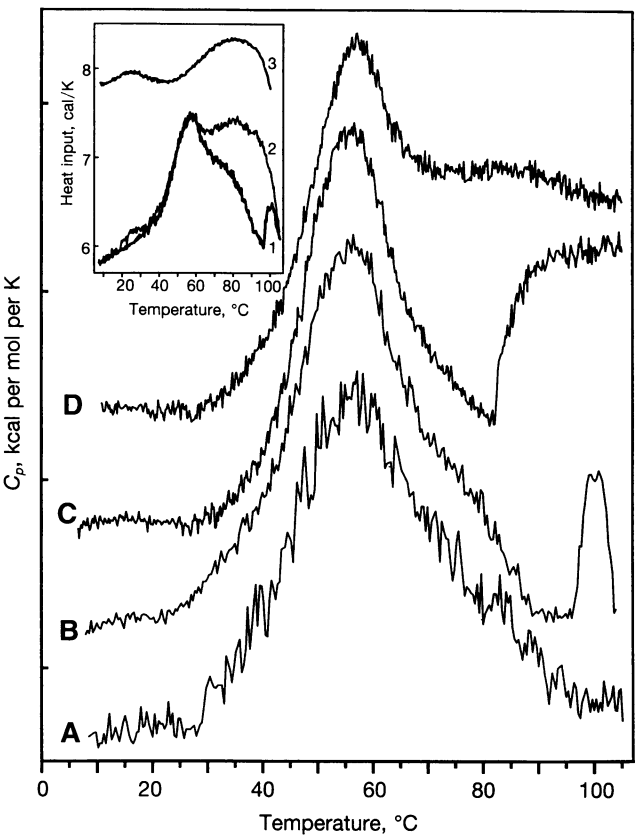

FIG. 1. Effect of apoA-1 concentration on the partial molar heat capacity $C_p(T)$. The data shown were recorded from four samples containing 0.01 M buffer at pH 7.2 with apoA-1 concentrations of 2.1 mg/ml (curve A), 4.7 mg/ml (curve B), 6.9 mg/ml (curve C), and 8.0 mg/ml (curve D). Buffer–buffer baselines were subtracted from the protein–buffer data, which were subsequently normalized to the protein concentration. Distance between the tick marks on the y axis is 1 kcal per mol per K; curves B–D are shifted along the y axis to avoid overlaps. The broad extent of the transition (25°C–90°C) results in low-amplitude changes in $C_p(T)$, leading to relatively low signal-to-noise ratio. Increase in the protein concentration from 2.1 mg/ml (curve A) to 4.7 mg/ml (curve B) increases the signal-to-noise ratio from 8 to 15 at the peak temperature of ≈57°C but leads to an additional high-temperature peak apparently resulting from aggregation of the thermally denatured protein. Further increase in the apoA-1 concentration leads to broadening of this additional peak, which merges with the thermal unfolding peak (curves C and D), thus interfering with the baseline determination for $C_p(T)$ integration. (*Inset*) Raw data recorded from 5°C to 105°C at a heating rate 90 degrees/h showing first (curve 1) and second (curve 2) consecutive scans of the sample containing apoA-1 (4.7 mg/ml) and buffer–buffer baseline (curve 3) that was subsequently subtracted from curve 1 to obtain curve B. Consecutive scans completely superimpose if the final heating temperature does not exceed 65°C. The differences between the first and subsequent scans occur upon heating the protein above 65°C (compare curves 1 and 2). These differences increase with increase in the number of the sample heatings or increase in the final heating temperature.

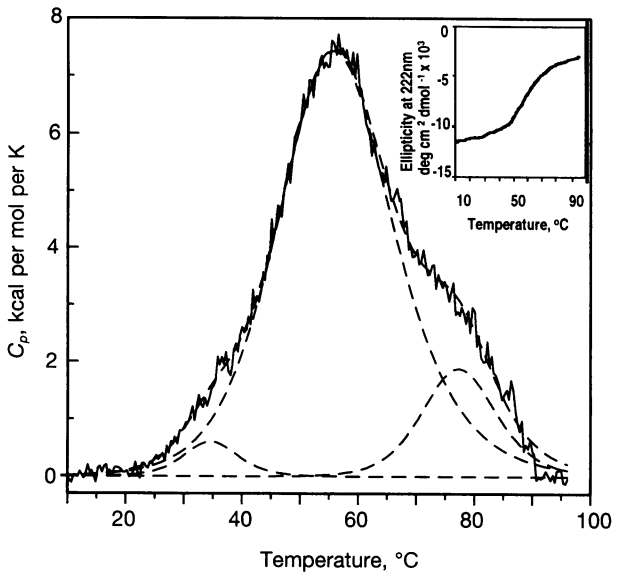

FIG. 2. Deconvolution of the heat capacity function $C_p(T)$. The baseline used for $C_p(T)$ integration was determined by extrapolating portions of the data recorded at 5°C–25°C and 90°C–96°C and was subtracted from curve B in Fig. 1. Thermal unfolding of apoA-1 is fitted by three consecutive non-two-state transitions (in dashed lines) of combined enthalpy $\Delta H_{cal} = 240 \pm 20$ kcal/mol. The major transition [$T_m = 57 \pm 1$°C, $\Delta H(T_m) = 200 \pm 20$ kcal/mol, $\Delta H_v(T_m) = 32.5 \pm 5$ kcal/mol] constitutes ≈80% of the total ΔH_{cal}. It is preceded by a small reversible transition [$T'_m \approx 35$°C, $\Delta H(T'_m) \approx 8$ kcal/mol], which is <5% of the total ΔH_{cal}, with the peak amplitude only about three times larger than the noise level. The major transition is followed by an irreversible transition [$T''_m \approx 78$°C, $\Delta H(T''_m) \approx 32$ kcal/mol], which occurs at a slower rate than the major transition. At a heating rate 90 degrees/h, this high-temperature transition constitutes ≈15% of the total ΔH_{cal}. (*Inset*) Melting of the α-helical structure in apoA-1 measured by the intensity of the 222-nm CD band. The data were recorded from a sample containing apoA-1 at a concentration of 0.18 mg/ml. Changes in the molar ellipticity are observed in the temperature range 25°C–90°C, with a first derivative maximum at $T_m \approx 58$°C.

temperatures below 25°C and above 90°C. A non-two-state model was used for the heat capacity deconvolution (Fig. 2), based upon our CD analysis that demonstrates the non-two-state character of apoA-1 unfolding (see *Results*). The model did not include oligomer disassociation, which was justified by the observed concentration independence of the peak temperature in the $C_p(T)$ function (Fig. 1). Attempts to incorporate disassociation in the analysis of the $C_p(T)$ function did not improve the quality of the fitting. The partial specific calorimetric ΔH and van't Hoff ΔH_v enthalpies of unfolding determined from the $C_p(T)$ data were independent of the buffer composition or protein concentration in the range of 1.7–4.7 mg/ml. The thermodynamic analysis in this work is based on the data collected from five protein samples at concentrations of 1.7–4.7 mg/ml.

CD Spectroscopy. Far-UV (184–250 nm) and near-UV (250–325 nm) CD spectra were measured with an Aviv Associates model 62DS spectrometer (Aviv Associates, Lakewood, NJ) equipped with a temperature controlling device and calibrated with camphorosulfonic acid. Spectra at six to eight constant temperatures were recorded from each protein and buffer sample, starting at 5°C and concluding at 90°C. The data were recorded every 0.5 nm at a rate of 0.5 nm/sec and averaged over five runs. The CD spectra were recorded in the far-UV by using a 0.5-mm quartz cell with apoA-1 at 0.17–0.3 mg/ml and in the near-UV by using a 10-mm cell with apoA-1 at 0.3–0.8 mg/ml. The normalized spectra were independent of the protein concentration. Thus, the observed temperature-dependent spectral changes were not linked to apoA-1 self-

association, which should be insignificant at concentrations ≤0.3 mg/ml (23).

RESULTS

Effect of apoA-1 Concentration on the Partial Heat Capacity $C_p(T)$. At protein concentrations of 1.7–4.7 mg/ml, the thermal transition of apoA-1 is resolved as a peak extending from 25°C to 90°C (Fig. 1, curves A and B). An additional high-temperature peak is observed at apoA-1 concentration >4 mg/ml (Fig. 1, curve B), apparently resulting from the aggregation of thermally denatured protein. With increase in apoA-1 concentration above 5 mg/ml, this additional peak broadens and shifts to lower temperatures overlapping the thermal transition (Fig. 1, curves C and D).

At apoA-1 concentrations <5 mg/ml, integration of $C_p(T)$ from 25°C to 90°C yields a total calorimetric enthalpy of ΔH_{cal} = 240 ± 20 kcal/mol (the error is largely due to the uncertainty in the baseline determination). High-temperature protein aggregation and the extent of the transition (which is close to the operating range, 5°C–105°C, of the MC-2 calorimeter) preclude accurate determination of ΔC_p. However, the calorimetric data recorded at protein concentrations <5 mg/ml show $\Delta C_p \leq 1$ kcal per mol per K. Comparison with the reported values ($\Delta H_{cal} \approx 64$ kcal/mol; $\Delta C_p = 2.4$ kcal per mol per K) estimated from the calorimetric data attained at apoA-1 concentrations of 7–40 mg/ml by using the integration range of 43°C–71°C (16, 17) suggests that high-temperature protein aggregation interfered with the baseline determination for $C_p(T)$ integration and led to an underestimate of ΔH_{cal} and overestimate of ΔC_p in refs. 16 and 17.

Thermodynamic Parameters of apoA-1 Unfolding. At apoA-1 concentrations <5 mg/ml, ≈80% of the total calorimetric enthalpy can be accounted for by a single reversible non-two-state transition with a midpoint temperature T_m = 57 ± 1°C, calorimetric enthalpy $\Delta H(T_m)$ = 200 ± 20 kcal/mol, and van't Hoff enthalpy $\Delta H_v(T_m)$ = 32.5 ± 5 kcal/mol (Fig. 2). The peak temperature of this major transition is close to the earlier calorimetric estimate of $T_m \approx 54$°C, and the van't Hoff enthalpy $\Delta H_v(T_m)$ can be compared with the range of 40–80 kcal/mol derived from the spectroscopic analysis of apoA-1 denaturation (16, 17).

The differences in the thermodynamic functions between the denatured and the native protein states at a reference temperature T_o can be calculated based on the measured difference in the heat capacities between these states ΔC_p and the calorimetric enthalpy $\Delta H(T_m)$, where T_m is the peak temperature assumed to be remote from T_o (24). The Gibbs free energy $\Delta G(T_o)$, enthalpy $\Delta H(T_o)$, and entropy $\Delta S(T_o)$ of unfolding are determined from the Gibbs–Helmholtz equation:

$$\Delta G(T_o) = \Delta H(T_m)(1 - T_o/T_m) + \Delta C_p[T_o - T_m + T_o \cdot \ln(T_m/T_o)] \quad [1]$$

or

$$\Delta G(T_o) = \Delta H(T_o) - T_o \cdot \Delta S(T_o),$$

where

$$\Delta H(T_o) = \Delta H(T_m) - \Delta C_p(T_m - T_o) \quad [2]$$

and

$$T_o \cdot \Delta S(T_o) = \Delta H(T_m) \cdot T_o/T_m - \Delta C_p \cdot T_o \cdot \ln(T_m/T_o). \quad [3]$$

The values of $\Delta H(T_o)$ and $\Delta S(T_o)$ for apoA-1 at T_o = 37°C were assessed, based on the calorimetric enthalpy $\Delta H(T_m)$ = 200 kcal/mol of the major transition, and assuming $\Delta C_p < 1$ kcal/mol. The leading terms in Eq. **2** [$\Delta H(T_m)$] and in Eq. **3** [$\Delta H(T_m) \cdot T_o/T_m$] constitute ≈90% of the total enthalpy and entropy changes, respectively. Neglecting the terms with ΔC_p in Eqs. **2** and **3** may lead to an ≈10% overestimate of ΔH(37°C) and ΔS(37°C). A small overestimate of these parameters might also result from proximity of T_o = 37°C to the broad peak with T_m = 57°C. Small errors may also arise from disassociation of apoA-1 oligomers that has not been accounted for in our analysis. With these assumptions, ΔH(37°C) = 200 kcal/mol = 7.2 cal/g, with an accuracy of ≈20%. Such accuracy is reasonable given the broad extent of the apoA-1 transition (compared to ≈5% error in the current estimates of the thermodynamic parameters of typical globular proteins that undergo highly cooperative unfolding).

CD Analysis of the Thermal Unfolding. Far- and near-UV CD spectra recorded at various stages of the thermal transition of lipid-free apoA-1 are shown in Figs. 3 and 4, respectively. The absence of a well-defined isochromatic point in the far-UV CD spectra (Fig. 3 *Inset*) suggests noncoincident melting of different secondary structural elements characteristic of a non-two-state transition (25). At near-physiological temperatures, the secondary structure of apoA-1 is largely intact (Fig. 3) and is characterized by ≈60% α-helical content, as inferred from the molar ellipticity at 222 nm measured in this and other studies (8, 11). Melting of the α-helical structure occurs between 25°C and 90°C, with midpoint $T_m \approx 58$°C (Fig. 2 *Inset*). In contrast, the tertiary contacts characterized by the intensities of the Tyr and Trp bands at 285 nm and 292 nm, respectively, are best defined at 5°C but appear largely melted at 40°C (Fig. 4). Thus, unfolding of the secondary structure of apoA-1 is preceded by the disruption of the tertiary contacts that at near-physiological temperatures are significantly melted.

DISCUSSION

Interpretation of the Calorimetric Transition. The peak temperature T_m and the calorimetric enthalpy $\Delta H_{cal}(T_m)$ of the major calorimetric transition are independent of the protein concentration (Fig. 1), even though apoA-1 is predominantly oligomeric at 25°C at the concentrations 1.7–4.7 mg/ml used in our calorimetric experiments (23). This suggests that the major transition may be due predominantly to the monomer unfolding rather than to disassociation of apoA-1 oligomers. Indeed, the extent (25°C–90°C) of the major calorimetric transition is in agreement with the range of melting of the α-helical structure determined by CD (Fig. 2 *Inset*). Since at ≈0.2 mg/ml concentrations used in the far-UV CD experiments apoA-1 is largely monomeric (23), the extended thermal transition can be attributed to the disruption of the secondary structure of the monomer rather than to quaternary structural changes. Furthermore, the midpoint $T_m \approx 57$°C of the calorimetric transition corresponds to the midpoint of melting of the α-helical structure (Fig. 2 *Inset*) which contains ≈60%, or ≈150 amino acids, in lipid-free apoA-1. The expected enthalpy of melting of this structure is ≈200 kcal/mol [using the value of 1.3 kcal/mol per residue for a random coil-to-helix transition in aqueous solution (26, 27)], in agreement with the measured $\Delta H(T_m)$ of the major calorimetric transition. Thus, this major transition may represent disruption of the α-helices in apoA-1. Comparison with the unfolding of isolated α-helices in water, which extends from ≈20°C to ≈100°C and is characterized by ≤20 residues in the cooperative unit (26), suggests that the α-helices in apoA-1 are relatively weakly stabilized by tertiary interactions.

The individual α-helices of apoA-1 may be stabilized by intrahelical salt links created by oppositely charged residue pairs located three or four positions apart. Eleven intrahelical salt links have been identified in the x-ray crystal structure of the N-terminal domain of human apolipoprotein E_3 (10). The amino acid sequence of apoA-1 contains 11 such residue pairs that may potentially contribute up to 70 kcal/mol to the

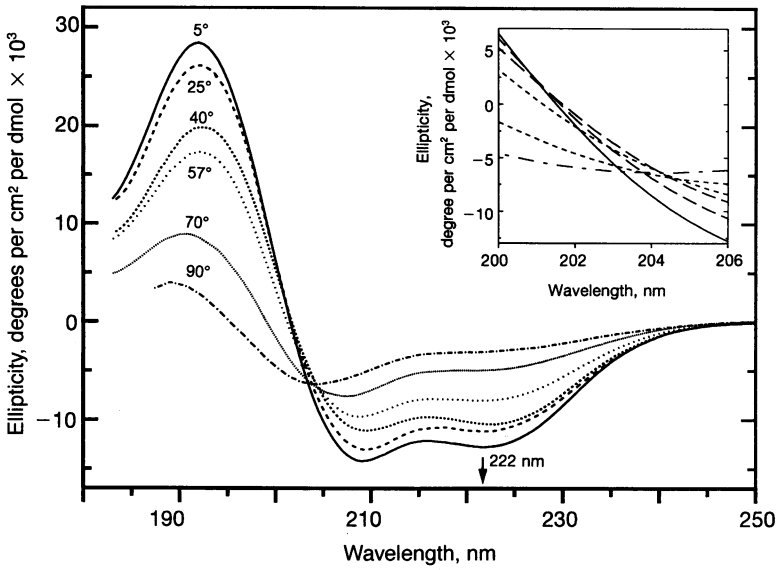

FIG. 3. Far-UV CD spectra of apoA-1 at different stages of the thermal unfolding. The series of spectra, recorded at several constant temperatures from a single sample containing apoA-1 (0.21 mg/ml) and 0.01 M buffer (pH 7.2), are shown. Lines: ——, 5°C; – – –, 25°C; - - - -, 40°C; · · · ·, 57°C; ·····, 70°C; · – · – ·, 90°C. (*Inset*) Enlarged view showing intersecting portions of the far-UV CD spectra. Absence of a well-defined isochromatic point indicates the non-two-state character of the thermal unfolding.

enthalpy of unfolding and compensate for the lack of tertiary interhelical stabilizing interactions.

The small low-temperature calorimetric transition ($T'_m \approx$ 35°C, $\Delta H(T'_m) \approx 8$ kcal/mol, and $\Delta H_v(T'_m) \approx 60$ kcal/mol) can be identified tentatively as the melting of the tertiary structure detected in this temperature range by near-UV CD (Fig. 4), which may be accompanied by disassociation of apoA-1 oligomers.

Comparison with Typical Globular Proteins. The partial specific enthalpy change for apoA-1 unfolding at 37°C and pH 7, estimated from our calorimetric data, is higher than the values of $\Delta H(37°C) \leq 5$ cal/g observed for midsize globular proteins, while the partial specific heat capacity change for apoA-1 ($\leq$0.035 cal/g) appears lower than the values of ΔC_p = 0.09–0.15 cal/g observed for the globular proteins (28). This suggests high polypeptide chain mobility of apoA-1, which for globular proteins is linked to increased $\Delta H(37°C)$ and reduced ΔC_p (28). Furthermore, the small ΔC_p apparently associated with apoA-1 unfolding indicates substantial exposure of nonpolar groups to water in the folded apolipoprotein state (29). High degree of solvent exposure of Tyr and Trp side chains in lipid-free apoA-1 has also been implied from near-UV absorption spectroscopy (15) and potentiometric titration (30). Solvent accessibility of apolar groups and the high polypeptide chain mobility inferred from these experiments are important for apoA-1 binding to HDL.

Molten Globular Characteristics of Lipid-Free apoA-1. The low cooperativity ($\Delta H_v/\Delta H \approx 0.16$) of the thermal unfolding of lipid-free apoA-1 and the temperature dependence of the far- and near-UV CD spectra indicate that the α-helixes of apoA-1 are only weakly stabilized by tertiary interactions. These features suggest a molten globular-like state for apoA-1

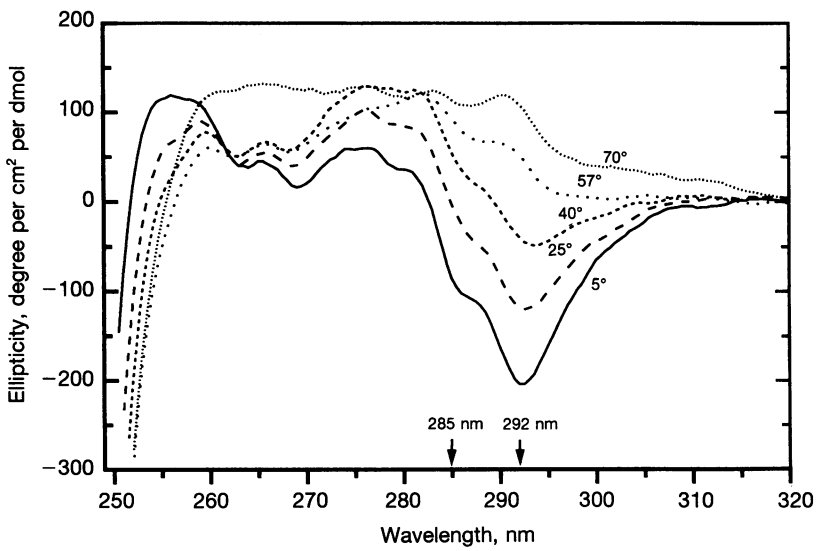

FIG. 4. Near-UV CD spectra of apoA-1 at different stages of the thermal unfolding. The spectra recorded at several constant temperatures from a single sample containing apoA-1 (0.31 mg/ml) and 0.01 M buffer (pH 7.2) are shown. Line coding is as in Fig. 3. The spectra at 70°C and 90°C (data not shown) significantly overlap. At 5°C, a well-defined negative trough with minima at 285 nm and 292 nm indicates orientational ordering of a significant fraction of the seven Tyr and four Trp groups present in apoA-1 sequence. Nearly 4-fold reduction in the depth of this trough at 40°C implicates substantial disruption of the tertiary structure at near-physiological conditions in plasma.

in low-salt solution at 37°C and pH 7. Several experimentally observed properties of lipid-free apoA-1 under near-physiological plasma conditions are consistent with the molten globular state: well-defined secondary structure (refs. 8 and 11 and this work) folded in a compact globular shape (12), low unfolding cooperativity (ref. 15 and this work), loose tertiary contacts and substantial solvent exposure of hydrophobic groups (refs. 15 and 30 and this work), affinity for hydrophobic ligands and tendency to aggregate (12, 23), and high susceptibility to denaturants (15, 16).

Stable molten globules have been observed *in vitro* for an increasing number of globular proteins under mild denaturing conditions (for review, see refs. 19, 25, and 31), and for synthetic α-helix bundle-forming peptides (32). The broad low-cooperativity unfolding characteristic of the molten globular state has limited the calorimetric analysis of this state to only a few cases (for review, see ref. 20). *In vivo*, molten globules stabilized by physiologically low pH have been inferred in the interactions of nascent proteins with chaperones and folding-assisting enzymes, in protein–membrane interactions, and in targeted release of nonpolar ligands from protein carriers (for review, see ref. 33). Our results suggest that apoA-1 represents another class of proteins whose main physiological function, namely lipid binding, may be mediated via the molten globular apolipoprotein state in plasma.

Transition of apoA-1 from the Lipid-Free to the HDL-Bound Form. Similar to the collapse of a molten globular to a tightly folded state (31), apoA-1 binding to HDL induces $\approx$15% increase in the α-helical content and enhances the protein stability against chemical and thermal denaturation (11). This enhanced stability is probably brought about by hydrophobic interactions between the apolar surfaces of the amphiphatic protein α-helices and the lipid matrix (7, 11). However, these lipid–protein interactions apparently lack the packing specificity characteristic of the internal protein side chains and do not present a high-energy barrier for apoA-1 exchange among HDL particles in the course of their metabolism (11). Thus, unfolding of apoA-1 on HDL may also be a complex non-two-state transition. This suggests that the enthalpies of unfolding of apoA-1 complexes with lipids, assessed from the spectroscopic analysis of their denaturation based on a two-state kinetic model (16, 34), may be underestimated.

Low free energies of stabilization $\Delta G \leq 4$ kcal/mol have also been inferred for other exchangeable apolipoproteins and their complexes with lipids [except the N-terminal domain of apoE (10)], based on the spectroscopic analysis of their chemical unfolding, which again was assumed to be a simple two-state process. However, sequence similarities of the members of this protein family (35) and their lipid binding and aggregation properties suggest that the lipid-free states of other exchangeable apolipoproteins may also be molten globular. If this is the case, then the thermodynamic parameters of unfolding of these apolipoproteins also have to be reevaluated.

We are grateful to Dr. Mary T. Walsh who introduced O.G. to the calorimetry and CD techniques, to Dr. Donald M. Small for useful discussions, to Dr. Donald L. D. Caspar for constructive criticism, and to Dr. Peter L. Privalov for valuable comments on the manuscript prior to publication. This work was supported by National Institutes of Health Grants HL26335 and HL48739 to D.A.

1. Brewer, H. B., Jr., Fairwell, T., Larue, A., Ronan, R., Houser, A. & Bronzert, T. J. (1978) *Biochem. Biophys. Res. Commun.* **80,** 623–630.
2. Karathanassis, S. K., Zannis, V. I. & Breslow, J. L. (1983) *Proc. Natl. Acad. Sci. USA* **80,** 6147–6151.
3. Fielding, C. J. & Fielding, P. E. (1981) *Proc. Natl. Acad. Sci. USA* **78,** 3911–3914.
4. Fielding, C. J., Shore, V. G. & Fielding, P. E. (1972) *Biochem. Biophys. Res. Commun.* **46,** 1943–1949.
5. Castelli, W. P., Doyle, J. T., Gordon, T., Hames, C. G., Hjortland, M. C., Hulley, C. B., Kagan, A. & Zukel, W. J. (1977) *Circulation* **55,** 767–772.
6. McLachlan, A. D. (1977) *Nature (London)* **267,** 465–466.
7. Segrest, J. P., Jones, M. K., De Loof, H., Brouilette, C. G., Venkatachalapathi, Y. V. & Anantharamaiah, G. M. (1992) *J. Lipid Res.* **33,** 141–166.
8. Nolte, R. T. & Atkinson, D. (1993) *Biophys. J.* **63,** 1221–1239.
9. Breiter, D. R., Kanost, M. R., Benning, M. M., Wesenberg, G., Law, J. H., Wells, M. A., Rayment, I. & Holden, H. M. (1991) *Biochemistry* **30,** 603–608.
10. Wilson, C., Wardell, M. R., Weisgraber, K. H., Mahley, R. W. & Agard, D. A. (1991) *Science* **252,** 1817–1822.
11. Atkinson, D. & Small, D. M. (1986) *Annu. Rev. Biophys. Biophys. Chem.* **15,** 403–456.
12. Barbeau, D. L., Jonas, A., Teng, T. & Scanu, A. M. (1979) *Biochemistry* **18,** 362–369.
13. Curtiss, L. K. & Edgington, T. S. (1985) *J. Biol. Chem.* **260,** 2982–2993.
14. Jonas, A., Wald, J. H., Toohill, K. L. H., Krul, E. S. & Kezdy, K. E. (1990) *J. Biol. Chem.* **265,** 22123–22129.
15. Reynolds, J. A. (1976) *J. Biol. Chem.* **251,** 6013–6015.
16. Tall, A. R., Shipley, G. G. & Small, D. M. (1976) *J. Biol. Chem.* **251,** 3749–3755.
17. Tall, A. R., Small, D. M., Shipley, G. G. & Lees, R. S. (1975) *Proc. Natl. Acad. Sci. USA* **72,** 4940–4942.
18. Gwynne, J., Brewer, B. & Edelhoch, H. (1974) *J. Biol. Chem.* **249,** 2411–2416.
19. Ptitsyn, O. (1992) in *Protein Folding*, ed. Creighton, T. E. (Freeman, New York), pp. 243–300.
20. Freire, E. (1995) *Annu. Rev. Biophys. Biomol. Struct.* **24,** 141–165.
21. Wetterau, J. R. & Jonas, A. (1982) *J. Biol. Chem.* **257,** 10961–10966.
22. Markwell, M. A. K., Haas, S. M., Bieber, L. L. & Tolbert, N. E. A. (1985) *Anal. Biochem.* **87,** 206–210.
23. Donovan, J. M., Benedek, G. B. & Carey, M. C. (1987) *Biochemistry* **26,** 8116–8125.
24. Privalov, P. L. & Khechinashvili, N. N. (1974) *J. Mol. Biol.* **86,** 665–684.
25. Kuwajiama, K. (1989) *Proteins* **16,** 87–103.
26. Privalov, P. L. (1982) *Adv. Protein Chem.* **35,** 1–104.
27. Sholtz, J. M., Marqusee, S., Baldwin, R. L., York, E. J., Stewart, J. M., Santoro, M. & Bolen, D. W. (1991) *Proc. Natl. Acad. Sci. USA* **88,** 2854–2858.
28. Privalov, P. L. (1979) *Adv. Protein Chem.* **33,** 167–241.
29. Privalov, P. L. & Makhatadze, G. I. (1990) *J. Mol. Biol.* **213,** 385–391.
30. Rosseneu, M., Soetewey, F., Lievens, M.-J., Vercaemst, R. & Peeters, H. (1977) *Eur. J. Biochem.* **79,** 251–257.
31. Haynie, D. T. & Freire, E. (1993) *Proteins* **16,** 115–140.
32. Handel, T. M., Williams, S. A. & De Grado, W. F. (1993) *Science* **261,** 879–885.
33. Bychova, V. E. & Ptitsyn, O. B. (1993) *Chemtracts Biochem. Mol. Biol.* **4,** 133–163.
34. Sparks, D. L., Lund-Katz, S. & Phillips, M. C. (1992) *J. Biol. Chem.* **267,** 25839–25847.
35. Li, W.-H., Tanimura, M., Luo, C.-C., Datta, S. & Chan, L. (1988) *J. Lipid Res.* **29,** 245–271.